

Thermal lensing in an end-pumped Yb:KGW slab laser with high power single emitter diodes

F. Hoos¹, S. Li¹, T. P. Meyrath¹, B. Braun² and H. Giessen¹

¹ *4. Physikalisches Institut, Universität Stuttgart, 70550 Stuttgart, Germany*

² *Georg-Simon-Ohm Hochschule, 90489 Nürnberg, Germany*

F.Hoos@physik.uni-stuttgart.de

Abstract: We demonstrate that it is possible to pump an N_g -cut Yb:KGW crystal slab with up to 18 W by a single emitter laser diode and still achieve a nearly diffraction limited output beam with a M^2 value below $M^2 < 1.1$ and optical to optical efficiencies of more than 44%. Furthermore, we have measured the focal length of thermally induced lenses in an Yb:KGW crystal slab which was end-pumped by 12 W and 18 W single-emitter diodes. We have observed that the focal lengths not only depend on the pump power and beam waists, but are also dependent on the specific diode beam profile, as well as the collimation optics. We have been able to correlate this behavior with specific patterns of the beam profile.

© 2008 Optical Society of America

OCIS codes: (230.6080) Optical devices, sources; (140.3480) Lasers, diode-pumped; (140.3615) Lasers, ytterbium; (140.6810) Thermal effects; (140.5560) Pumping.

References and links

1. G. R. Holtom, "Mode-locked Yb:KGW laser longitudinally pumped by polarization-coupled diode bars," *Opt. Lett.* **31**, 2719–2721 (2006).
2. A. A. Lagatsky, C. T. A. Brown, and W. Sibbett, "Highly efficient and low threshold diode-pumped Kerr-lens mode-locked Yb:KYW laser," *Opt. Express* **12**, 3928–3933 (2004).
3. J. E. Hellström, S. Bjurshagen, V. Pasiskevicius, J. Liu, V. Petrov, and U. Griebner, "Efficient Yb:KGW lasers end-pumped by high-power diode bars," *Appl. Phys. B* **83**, 235–239 (2006).
4. EKSPLA, "Yb:KGW and Yb:KYW Crystals," <http://www.ekspla.com/en/main/products/1/63?pid=498>.
5. I. V. Mochalov, "Nonlinear optics of the potassium gadolinium tungstate laser crystal $\text{Nd}^{3+}:\text{KGd}(\text{WO}_4)_2$," *J. Opt. Technol.* **62**, 746–756 (1995).
6. C. Hönninger, R. Paschotta, M. Graf, F. Morier-Genoud, G. Zhang, M. Moser, S. Biswal, J. Nees, A. Braun, G. A. Mourou, I. Johannsen, A. Giessen, W. Seiber, and U. Keller, "Ultrafast ytterbium-doped bulk lasers and laser amplifiers," *Appl. Phys. B* **69**, 3–17 (1999).
7. F. Brunner, T. Südmeyer, E. Innerhofer, F. Morier-Genoud, and R. Paschotta, "240-fs pulses with 22-W average power from a mode-locked thin-disk Yb:KY(WO₄)₂ laser," *Opt. Lett.* **27**, 1162–1164 (2002).
8. T. Kawashima, T. Kurita, O. Matsumoto, T. Ikegawa, T. Sekine, M. Miyamoto, K. Iyama, H. Kan, and Y. Tsuchiya, "20-J Diode-Pumped Zig-Zag Slab Laser with 2-GW Peak Power and 200-W Average Power," ASSP 2005, TuB44 (2005).
9. G. Erbert, G. Beister, R. Hülsewede, A. Knauer, W. Pittroff, J. Sebastian, H. Wenzel, M. Weyers, and G. Tränkle, "High-Power Highly Reliable Al-Free 940-nm Diode Lasers," *IEEE J. Sel. Top. Quantum Electron.* **7**, 143–148 (2001).
10. J. Sebastian, G. Beister, F. Bugge, f. Buhrandt, G. Erbert, G. Hänsel, R. Hülsewede, A. Knauer, W. Pittroff, R. Staske, M. Schröder, H. Wenzel, M. Weyers, and G. Tränkle, "High-Power 810-nm GaAsP-AlGaAs Diode Lasers With Narrow Beam Divergence," *IEEE J. Sel. Top. Quantum Electron.* **7**, 334–339 (2001).
11. G. Erbert, A. Bärwolff, J. Sebastian, and J. Tomm, "High-Power Broad-Area Diode Lasers and Laser Bars," *Topics Appl. Phys.* **78**, 172–223 (2000).

12. A. E. Siegman, *Lasers*, (University Science Books, 1986).
13. S. Chénais, F. Balembois, F. Druon, G. Lucas-Leclin, and P. Georges, "Thermal Lensing in Diode-Pumped Ytterbium Lasers - Part I: Theoretical Analysis and Wavefront Measurements," *IEEE J. Quantum Electron.* **40**, 1217–1234 (2004).
14. J. E. Hellström, S. Bjurshagen, and V. Pasiskevicius "Laser performance and thermal lensing in high-power diode-pumped Yb:KGW with athermal orientation," *Appl. Phys. B* **83**, 55–59 (2006).
15. G. Wagner, M. Shiler, and V. Wulfmeyer, "Simulations of thermal lensing of a Ti:Sapphire crystal end-pumped with high average power," *Opt. Express* **13**, 8045–8055 (2005).
16. H. Ibach and H. Lüth, *Solid-State Physics*, (Springer, 2003).
17. S. Biswal, S. P. O'Connor, and S. Steven, "Thermo-optical parameters measured in ytterbium-doped potassium gadolinium tungstate" *Appl. Opt.* **44**, 3093–3097 (2005).
18. A. A. Lagatsky, A. Abdolvand, and N. V. Kuleshov, "Passive Q switching and self-frequency Raman conversion in a diode-pumped Yb:KGd(WO₄)₂ laser," *Opt. Lett.* **25**, 616–618 (2000).
19. S. Biswal, S. Shawn, P. O'Connor, and S.R. Bowman, "Thermo-optical parameters measured in potassium-gadolinium-tungstate," *CLEO 2004, CThT62* (2004).
20. V. V. Filippov, N. V. Kuleshov, and I. T. Bodnar, "Negative thermo-optical coefficients and athermal directions in monoclinic KGd(WO₄)₂ and KY(WO₄)₂ laser host crystals in the visible region," *Appl. Phys. B* **87**, 611–614 (2007).
21. S. Chénais, F. Druon, S. Forget, F. Balembois, and P. Georges, "On thermal effects in solid state lasers: the case of ytterbium-doped materials," <http://arxiv.org/ftp/arxiv/papers/0704/0704.0701.pdf>.
22. C. E. Mungan, "Thermodynamics of radiation-balanced lasing," *J. Opt. Soc. Am. B* **20**, 1075–1082 (2003).

1. Introduction

A promising approach towards compact multi-watt femtosecond supercontinua is offered by directly diode-pumped Ytterbium doped tungstate lasers (e.g. Yb:KGW or Yb:KYW) [1, 2, 3]. Ytterbium doped tungstates offer high emission and absorption cross sections leading to very high efficiencies while the emission spectrum is still sufficiently broad to support femtosecond pulses [2]. With a thermal conductivity between 2.6 and 3.8 W/m·K [4, 5], ranging between those of laser glasses (0.85-1.30 W/K·m) and highly conducting materials such as YAG (14 W/m·K) [6], Ytterbium doped tungstates can be used to achieve average powers of several tens of watts [7].

One important challenge of pumping laser crystals with high power diodes is the evolution of a non-uniform heat distribution inside the crystal. The temperature distribution changes the index of refraction and causes mechanical strains and stresses. Both effects lead to a change of the optical properties of the laser crystal. Some of the effects can be compensated by a suitable resonator design, whereas higher-order aberrations often lead to a low output beam quality. Especially for mode-locked lasers, it is important to minimize higher-order aberrations in order to assure a nearly diffraction limited beam quality. In order to overcome spatial variations of the optical path length due to a non-uniform heat distribution, various schemes have been pursued. Very high average power femtosecond lasers can be achieved with thin-disk lasers [7] where the heat is transferred collinearly with the propagating laser beam or by zig-zag geometry slab lasers [8] where the optical path length is averaged over the whole laser mode beam profile. When propagating straight through a slab crystal, it is important to assure an approximately parabolic change in the index of refraction in order to avoid higher-order aberrations. This can be achieved by carefully choosing the laser crystal geometry and pump laser diodes as well as the pump optics.

In the recent years, bulk lasers with straight beam propagation have made significant advances mostly due to new laser host materials such as Ytterbium doped tungstates and the availability of high quality pump diodes [1, 3]. A further advance is possible by the application of high power single emitter diodes [9, 10] which can provide more than ten watts of pump power out of a single emitter. In one direction, the beam profile of these diodes consists of a pattern of many transversal modes, whereas it is nearly diffraction limited in the other direction [9, 10, 11].

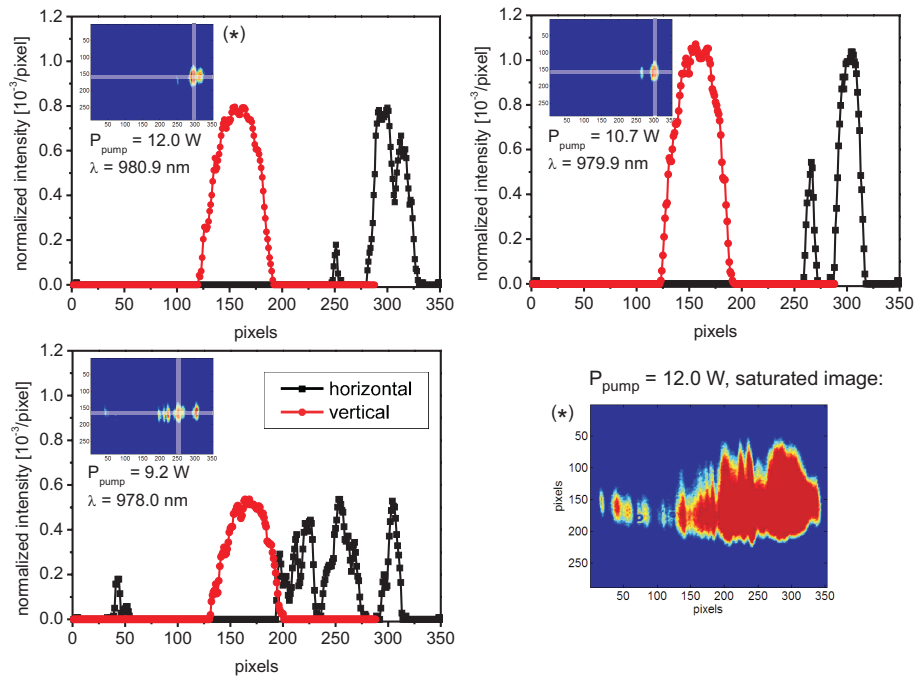


Fig. 1. Cross section plots of the normalized intensity of beam profiles of a 12 W single emitter diode operating at various power settings. The beam profiles were taken with a CCD camera at output powers between 9.2 W and 12.0 W as indicated. The red curves (circles) depict the beam profile along the vertical axis and the black curves (squares) along the horizontal axis. The linear plots approximately depict the area taken into account with calculations with the M^2 -parameter, whereas the lower right plot shows a saturated image at 12 W to emphasize the overall area covered by the beam profile.

While the formation of a thermal lens in Ytterbium doped tungstates has already been the subject of contemporary research [13, 14], we have discovered that the thermal lensing is somewhat different from what one might expect when end-pumping with high power single emitter diodes. In this paper, experimental results of thermal lensing when end-pumping an Yb:KGW crystal with a 12 W and a 18 W single emitter diode are presented and the influence of the particular beam profiles is discussed. These results are compared with simulations and a suggestion is made as to take the beam profile of single-emitters into account when estimating the behavior of the thermal lens.

2. Experimental results

All experiments were carried out by pumping a flat Brewster-cut slab of KGW doped with 1 at.% Ytterbium. The optical path length inside the 5 mm broad N_g -cut crystal is 7 mm and its height is 1.2 mm. The crystal is mounted with the two broad surfaces between two copper blocks and the gaps are filled with indium foil to improve the thermal contact. The heat flow is oriented parallel to the crystallographic b -axis to ensure the best thermal conductivity. The flat side of the crystal is anti-reflection coated at the pump wavelength 981 nm and for the laser wavelength around 1030 nm. At 981 nm, approximately 95% of the pump light is absorbed under non-lasing conditions, whereas away from the center wavelength the absorption

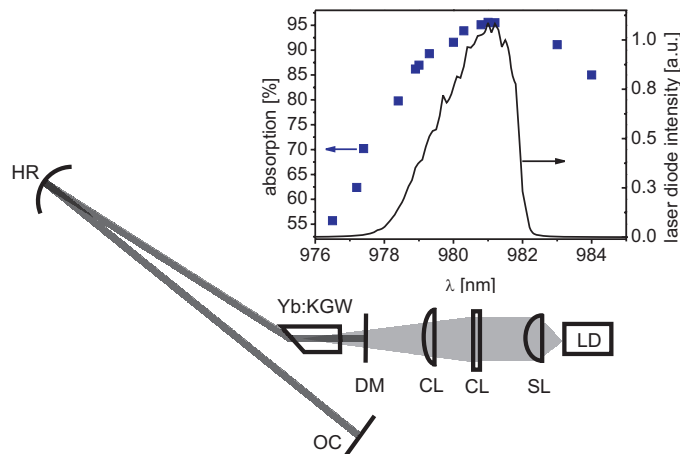


Fig. 2. The focal length of the thermal lens was determined by measuring the divergence angle of the output laser beam of a three-mirror cavity. Here LD denotes the single emitter laser diode, SL and CL are one spherical and two cylindrical lenses, respectively, DM is a dichroic mirror, HR is a curved highly reflective mirror, and OC is a output coupling mirror. The plot gives the wavelength dependence of the pump light absorption in the Yb:KGW crystal for non-lasing conditions and a sample spectrum of a 12 W single emitter diode.

is reduced (inset of Fig. 2).

As high power single emitters, we use in our experiments a 12 W and a 18 W InGaAs MQW broad area emitter at 981 nm (Ferdinand-Braun-Institut für Höchstfrequenztechnik (FBH), Berlin). The beam is emitted from a 200 μm wide emitter with a waveguide thickness of approximately 3 μm . The output beam is first collimated with an aspheric lens with $f=3.1$ mm focal length and then refocused into the laser medium with two cylindrical lenses with $f=200$ mm and $f=50$ mm focal length, respectively. The beam size inside the crystal was calculated to be approximately 400 μm by 210 μm in diameter at the front surface of the crystal.

The beam profile of the pump diodes was nearly diffraction limited in the vertical direction but showed a pattern with a series of minima and maxima in the horizontal direction. The beam quality was estimated to be approximately $M^2=1.2$ in the vertical and $M^2=50$ in the horizontal direction in the case of the 12 W and $M^2=60$ in the case of the 18 W diode, respectively. The unique horizontal pattern is dependent on the specific laser diode, the feedback from the collimation optics due to back reflections, and the of the laser diode. Fig. (1) shows the normalized intensity of beam profiles of a 12 W single emitter diode. The images were taken for various output powers with a CCD camera using an AR coated collimation lens with a focal length of $f=3.1$ mm. The linear images depict the are that is taken into account by an approximation with the M^2 -parameter [12]. However, as shown later, for the calculation of the thermal lens it is important to take the specific beam profile and the full covered area into account. The lower right plot of Fig. (1) shows a saturated image taken at the highest output power of 12 W to exhibit the full covered area of the beam profile. As one can further see, the beam is nearly Gaussian distributed along the vertical direction, whereas the beam profile along the horizontal axis has a more complex pattern due to the superposition of many transversal modes.

In order to measure the thermal lens and to demonstrate the possibilities of this arrangement of crystal orientation and specific pump diodes, several end-pumped three-mirror cavities were build around the laser crystal (Fig.2). The divergence angle of the laser beam is measured at the

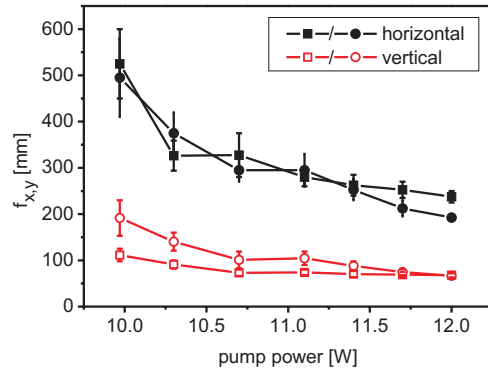


Fig. 3. The focal length of the thermal lens along two axes induced by end pumping the Yb:KGW crystal with a 12 W single emitter diode was determined experimentally by measuring the beam divergence of the output beam of two different three-mirror laser resonators (squares: resonator with a curved mirror with 200 mm radius, circles: resonator with a mirror with a radius of curvature of 300 mm).

output coupling mirror with a beam propagation analyzer (Coherent, Modemaster). The divergence angle can then be compared with theoretical results of a simulation of the resonator with beam propagation matrices [12]. Fig. 3 shows the obtained focal lengths for the thermal lens in the horizontal and vertical direction. The results were obtained by measuring the divergence angle of two different resonators. The resonators varied in the radius of the curved mirror and in the length of the two long arms. The first resonator used a curved mirror with a radius of 200 mm whereas the second resonator employed a mirror with a radius of 300 mm. In both resonators, the crystal was end-pumped with a 12 W diode. As error sources, only the error of the divergence angle measurement and the angle of incidence on the curved mirror were taken into account. All data points used to calculate focal lengths of thermal lenses were selected only when the beam quality was below $M^2 < 1.2$.

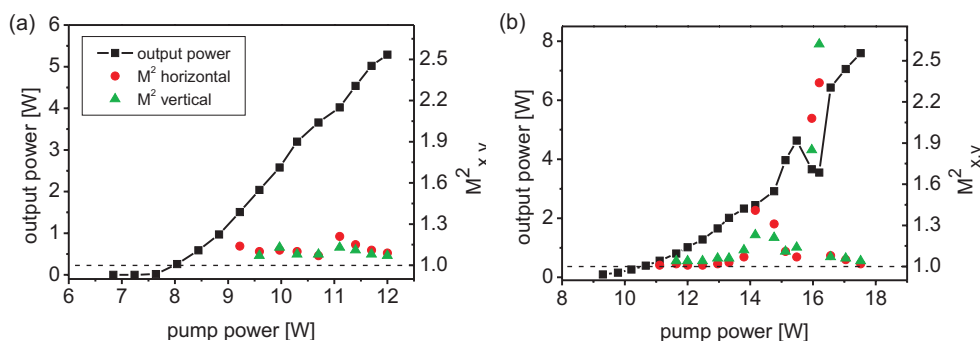


Fig. 4. Output power (black curve, squares) and M^2 -values (circles horizontal and triangles vertical) for resonators pumped with a 12 W diode (a) and with a 18 W diode (b), respectively. The laser wavelength was approximately 1030 nm for all pump powers and the pump wavelength ranged from approximately 976 nm to 981 nm for the highest pump power.

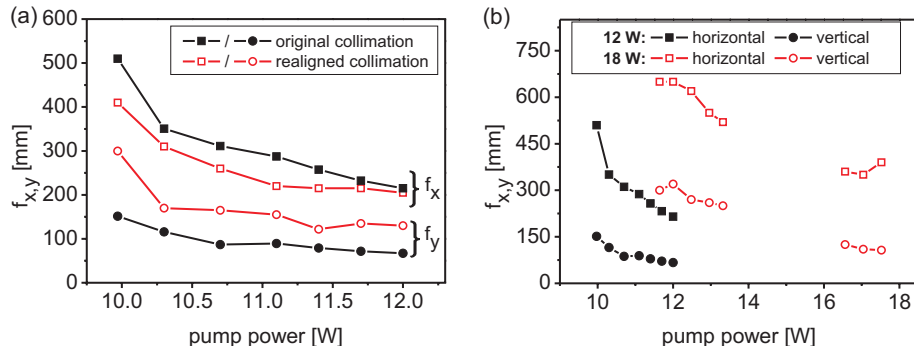


Fig. 5. (a) Measurements of the thermal lens with the same diode. The full symbols depict the focal length for the original collimation and the hollow symbols for a slightly realigned collimation lens (squares: horizontal, circles: vertical direction). (b) Thermal lens with 12 W and 18 W diodes. Even if the beam diameters were held the same in both cases, the thermal lens is stronger in the case of *less* pump power (squares: horizontal, circles: vertical, full symbols: 12 W diode, hollow symbols: 18 W diode).

All laser resonators that were used to determine thermal lenses had a high efficiency and good beam quality. The maximum optical to optical efficiency in cw-operation was 44% in the case of pumping with the 12 W diode resulting in 5.3 W output power, and 43% in the case of pumping with 18 W, resulting in 7.7 W output power. The beam quality parameter M^2 was kept below $M^2 < 1.1$ for the highest pump powers in each configuration (Fig. 4). Reducing the horizontal beam diameter do half the size as before and keeping the vertical diameter constant increased the M^2 -value to $M^2=2.03 \times 1.07$ at an optical to optical efficiency of $\eta=48\%$ when pumping with the 12 W diode.

To consider the influence of the beam profile, Fig. 5 (b) shows the focal lengths of the thermal lens by pumping with the same 12 W diode and an 18 W diode for comparison. To measure the thermal lens we used the two different three mirror cavities in the case of the 12 W diode but a more complex cavity in the case of the 18 W diode. However, the pump optics and all beam diameters inside the laser crystal remain. Surprisingly, the 18 W diode induces a weaker thermal lens than the 12 W diode, which is, in fact, due to the differences in their beam profiles.

In order to test the influence of the pump optics, the thermal lens was measured with the same 12 W diode but a slightly re-aligned collimation lens. All lenses and distances were held constant. Fig. 5 (a) shows the results of this measurement in comparison to the aforementioned results. The re-alignment of the collimation optics caused the thermal lens to become stronger horizontally and weaker vertically.

3. Theoretical model

In order to further investigate the experimental observations and the influence of the beam profile on the thermal lens, the heat distribution inside the laser crystal was simulated and the focal length of the thermal lens could be derived as by the method of reference [15]. The stationary heat distribution was calculated by the heat equation

$$-\nabla[k(T)\nabla T(\mathbf{r})] = \mathbf{Q}(\mathbf{r}), \quad (1)$$

where $T(\mathbf{r})$ is the spatial temperature distribution, $\mathbf{Q}(\mathbf{r})$ is the heat source, and $k(T)$ is the temperature dependent thermal conductivity. In the case of KGW, k is a tensor [4, 5]. The

temperature dependence of k was modeled with a $1/T$ behavior as expected for temperatures above 100 K [16]. The crystal was clamped with its broad surfaces between two copper blocks, and the gap was filled with 50 μm indium foil. The heat transfer coefficient from the crystal to the copper block was assumed to be 9000 $\text{W}/\text{m}^2\text{K}$ [21]. Figure 7 shows cross sections of the temperature profile at the center of the crystal front surface. By using the thermo-optic coefficient, $\partial n/\partial T$, a spatial distribution of the refractive index was obtained. The thermo-optic coefficient is a parameter which, as yet, remains imprecisely known for Yb:KGW. The values in the literature vary from $4.3 \cdot 10^{-6}\text{K}^{-1}$ to $-1.0 \cdot 10^{-5}\text{K}^{-1}$ [5, 17]. For our case, with the laser light polarization along the crystallo-optic N_m -axis, we chose values close to $0.4 \cdot 10^{-6}\text{K}^{-1}$ based on crystal manufacturer's specifications [4] as well as on several references [18, 19, 20]. However, to also take the photo-elastic effect into account we used $0.2 \cdot 10^{-6}\text{K}^{-1}$ along the N_m -axis and $0.9 \cdot 10^{-6}\text{K}^{-1}$ along the b -axis. The temperature profile was then fit in the horizontal as well as in the vertical direction by a parabolic function for each of 200 slices along the propagation axis. With the parabolic fits, the focal length of the thermal lens was derived using the procedure in reference [15].

Furthermore, the bulging of the crystal surface due to the inhomogeneous heat distribution was taken into account. The influence on the optical properties was modeled by a parabolic lens. By fitting a parabolic function to the displacement of the crystal surface (Fig. 7), the focal length of this contribution was derived by the relation

$$f = \frac{1}{(n-1) \cdot 2A}, \quad (2)$$

where $2A$ denotes the curvature of the parabola and n the index of refraction. As thermal expansion coefficients we used the values given by the crystal manufacturer [4] which are also very close to the ones given by reference [5]. Young's modulus was taken from [5] and the Poisson's ratio was estimated to be approximately $\nu = 0.3$.

The minimum amount of pump power that is transferred to heat was estimated to be approximately 49% during laser operation. This estimate was based on the 44% maximum optical to optical efficiency by pumping the laser with the 12 W diode and 7% further losses for instance due to residual reflections at the crystal surfaces during measurement.

Figure 7 shows the resulting focal lengths obtained from the simulation for two different scenarios and for two different types of pump diodes. Figure 7 (b) shows the results for thermal

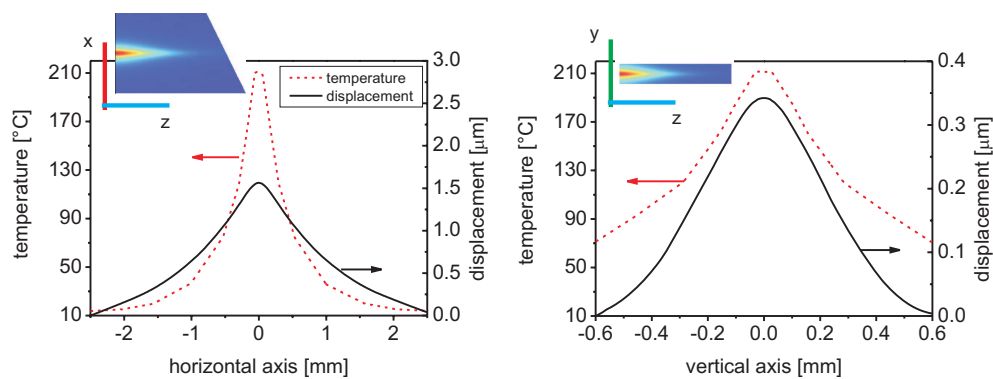


Fig. 6. The temperature distribution inside the laser crystal and the bulging of the front facet was simulated by finite element analysis. The diagrams depict the results for 12 W pump power with a Gaussian beam profile without mode pattern. The insets show the temperature distribution in two perpendicular planes through the crystal.

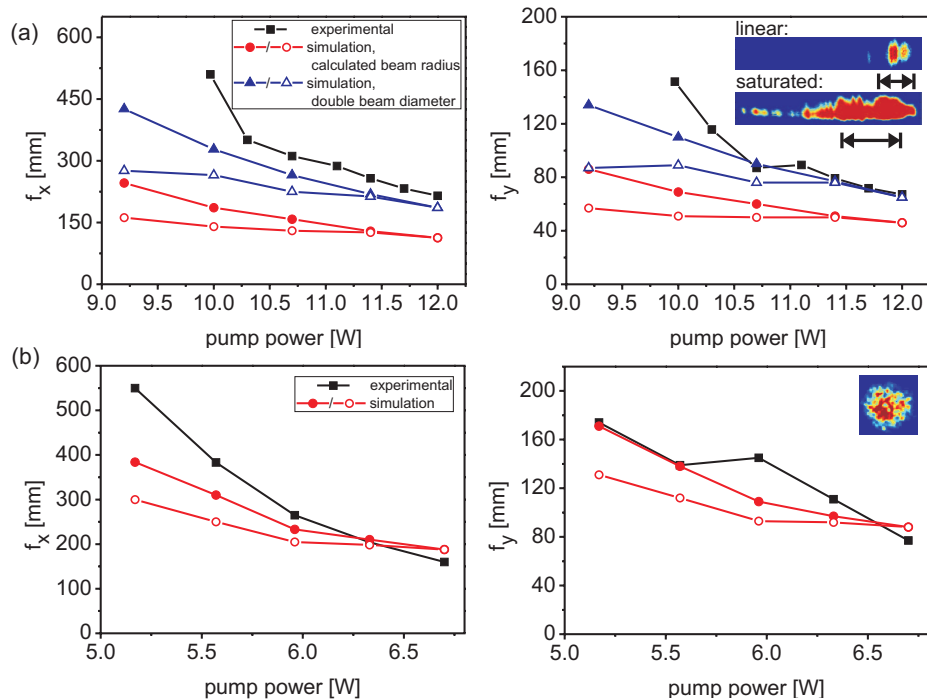


Fig. 7. (a) Focal length of the thermal lens when pumping with a 12 W single emitter diode and for pumping with a multi-mode fiber-coupled 6.7 W diode with $M^2=24 \times 24$ (b), respectively. The black curves (squares) show experimental data points, whereas the red curves (circles) were obtained theoretically with a Gaussian beam profile with the calculated diameter. The blue curves (triangles) show theoretical data obtained for a Gaussian beam profile with twice the calculated beam diameter. Full symbols depict simulations with a fixed fraction of pump light converted to heat, whereas the hollow symbols take the laser efficiency into account. The inset images show the pump beam profiles of each pump diode.

lenses induced by pumping with a multimode fiber-coupled 6.7 W laser diode. The pump spot was circular in this case and the diameters were held at $w_p = 110 \mu\text{m}$. The maximum absorption amounted to 75% due to the different polarization. Figure 7 (a) shows the results for pumping with a 12 W single emitter diode.

The hollow symbols depict the simulations when taking the laser efficiency into account and assuming all residual absorbed pump power which is not converted to laser light as a heat load. The full symbols show the results if one assumes the fraction of pump light which is converted to heat to be fixed at 49%. Each simulation additionally takes into account the appropriate absorption coefficient. All values were calculated for pumping the laser with the 12 W diode. The second scenario with a fixed fraction of pump light as heat source seems to fit the realistic situation better. This could be due to a stimulated excitation of anti-Stokes Raman scattering which leads to a conversion of pump power to fluorescence light instead of heat [22]. Yb:KGW is known to show strong Raman shifts [18]. Another reason for the deviation for pump powers below 10.5 W could be that some part of the losses are due to re-absorption of laser light. This absorption would be homogeneously distributed over the full crystal length as opposed to the exponentially decaying pump light. The simulation model remains relatively simple and many material parameters are not considered or imprecisely known.

The red curves (circles) in Fig. 7 show the result if one takes the beam profile into account according to manufacturer specifications and the appropriate M^2 value. The blue curves (triangles) show the theoretical results if one assumes twice the beam diameter in the horizontal direction in order to account for the full covered area. In both cases simple Gaussian distributions but different horizontal beam diameters were assumed.

To compare these results with the experiment, the black curves (squares) show the experimental data. We recognize that for the case when pumping with the single emitter (Fig. 7 (a)), the measured focal lengths agree better with the ones obtained theoretically with twice the horizontal beam diameter.

The N_g -cut crystal orientation does not allow for an athermal orientation such as in [14, 20]. The thermo-optic coefficient $\partial n/\partial T$ is very close to zero but still positive. Therefore, the thermo-optic and photo-elastic effects cannot compensate for the bulging of the crystal surface. However, when pumping with more than 10 W the focal lengths are still reasonably large and the change of optical path length can be very well fit by a parabolic function. Therefore, it is possible to compensate the thermal effects.

4. Conclusion

We have demonstrated that it is possible to pump an N_g -cut KGW crystal slab with up to 18 W out of a single emitter laser diode and still achieve a nearly diffraction limited output beam with an M^2 below 1.1 and efficiencies of more than 44%.

Furthermore, we have presented experimental values for the focal length of thermal lenses by end-pumping a long Yb:KGW slab with high power single emitter diodes. While the beam diameters for the overlap with the laser mode can be calculated with the M^2 -value, one finds experimentally that the thermal lens strongly depends on the specific diode used as well as on the collimation optics, which are usually in close proximity to the diode facet causing small back reflections. By comparing images of the beam profiles of the same pump diode for various pump powers and by comparing the experimental values with those theoretically obtained, we come to the conclusion that it is crucial to not only take the diode parameters such as M^2 value, but also the beam profile and the full covered area of the specific combination of diode and collimation optics into account. For a very precise determination of the thermal lens under end-pumping with high power single emitter diodes, it is important to make measurements with each combination of diode and pump optics or assure a similar beam profile when assembling the combinations.

Since high power single emitter diodes provide cost-effective high power pump sources with an outstanding beam quality, they allow for the development of high power femtosecond bulk lasers. This work will aid in the development of suitable pump optics and laser resonators for high power femtosecond laser oscillators that are pumped with single emitter diodes.

Acknowledgments

The authors would like to thank Dr. Götz Erbert of the Ferdinand-Braun-Institut für Höchstfrequenztechnik, Berlin, for supplying us with high power single emitter diodes and many valuable advice. Furthermore, we would like to thank the DFG (FOR557, FOR730) and the BMBF (13N8340/1) for support. T.P. Meyrath acknowledges the support from the Alexander von Humboldt foundation.